Optics Letters

Phase-matched electric-field-induced second-harmonic generation in Xe-filled hollow-core photonic crystal fiber

JEAN-MICHEL MÉNARD* AND PHILIP ST.J. RUSSELL

Max Planck Institute for the Science of Light, Günther-Scharowsky Straße 1, 91058 Erlangen, Germany
**Corresponding author: jean-michel.menard@mpl.mpg.de*

Received 2 June 2015; revised 14 July 2015; accepted 15 July 2015; posted 15 July 2015 (Doc. ID 242141); published 31 July 2015

Second-order nonlinearity is induced inside a Xe-filled hollow-core photonic crystal fiber (PCF) by applying an external dc field. The system uniquely allows the linear optical properties to be adjusted by changing the gas pressure, allowing for precise phase matching between the LP_{01} mode at 1064 nm and the LP_{02} mode at 532 nm. The dependence of the second-harmonic conversion efficiency on the gas pressure, launched pulse energy, and applied field agrees well with theory. The ultra-broadband guidance offered by anti-resonant reflecting hollow-core PCFs, for example, a kagomé PCF, offers many possibilities for generating light in traditionally difficult-to-access regions of the electromagnetic spectrum, such as the ultraviolet or the terahertz windows. The system can also be used for non-invasive measurements of the transmission loss in a hollow-core PCF over a broad spectrum, including the deep and vacuum UV regions.

OCIS codes: (060.5295) Photonic crystal fibers; (190.4223) Nonlinear wave mixing; (230.7405) Wavelength conversion devices; (060.2270) Fiber characterization.

http://dx.doi.org/10.1364/OL.40.003679

The hollow-core photonic crystal fiber (PCF) provides a convenient platform for exploring nonlinear optical effects in gases [1–4]. The combination of long optical path lengths, pressure-adjustable dispersion, and tight field confinement means that nonlinear processes can be highly efficient, even though gases have smaller nonlinear coefficients than silica (~100 times lower at ambient pressure and temperature [5,6]). To date, many experiments have been reported that make use of the intrinsic third-order nonlinearities of gases (including, if appropriate, the Raman response), augmented at high field intensities by ionization-driven nonlinear effects [7–10].

Structurally amorphous media such as gases or glasses are macroscopically inversion symmetric, with vanishingly small values of second-order susceptibility $\chi^{(2)}$. If, however, a dc electric field E_{dc} is applied, the centrosymmetry can be broken and nonzero values of $\chi^{(2)} \propto \chi^{(3)} E_{dc}$ can be induced. This process has been extensively studied in conventional step-index fibers, where the noninversion symmetry can be created either by direct electric field poling or by mixing the pump and second-harmonic (SH) signals so as to create a dc polarization via $\chi^{(3)}(0{:}\omega + \omega - 2\omega) E_{\omega}^{2} E_{2\omega}^{*}$ [11,12].

Here, we report experiments in which $\chi^{(2)}$ is induced in a Xe-filled kagomé PCF by applying a uniform dc electric field across its core. Note that $\chi^{(3)}$ in Xe scales linearly with pressure (up to ~20 bar), equaling 2.03×10^{-25} m^2/V^2 at 1 bar [5]. Phase-matching between the LP_{01} pump and the LP_{02} SH modes can be obtained over a broad range of pump wavelengths simply by varying the gas pressure, as seen in Fig. 1(a), where the modal refractive indices (calculated using the expressions in [1,13,14]) are plotted against the wavelength for a Xe pressure of 4.35 bar. The difference between the modal indices of the LP_{01} pump (n_{ω}) and the LP_{02} SH ($n_{2\omega}$) is displayed as a function of both the pressure and pump wavelength in Fig. 1(b). Notably, a 1.3 bar change in Xe pressure shifts the phase-matching wavelength by 100 nm.

Figure 2 shows a schematic of the experimental setup, together with a scanning electron microscope (SEM) image of the kagomé PCF structure. Planar electrodes 16 cm long were placed on opposite sides of the fiber (total length 45 cm, and outer diameter 264 μm), and a 100 μm-thick polyvinyl chloride (PVC) film was inserted between them, directly under the PCF, so as to avoid electrical breakdown at the maximum applied voltage V_{app} of 1.8 kV. Taking account of the diameter of the air-like photonic crystal cladding (170 μm), the thickness of the encircling silica sheath (47 μm), and the dielectric constants of the silica (3.8) and the PVC (3.2), we estimate the field in the core to be $E_{dc} = 44 \times V_{app}$ V/cm. So as to avoid charge screening effects, which for dc fields were found to be very strong (the reason for this is not yet clear), a 350 Hz square-wave ac electric field with zero mean voltage was used.

A Xe pressure of 4.35 bar was chosen to satisfy the phase matching between an LP_{01} pump at 1064 nm and an LP_{02} SH at 532 nm [this corresponds to the situation in Fig. 1(a)].

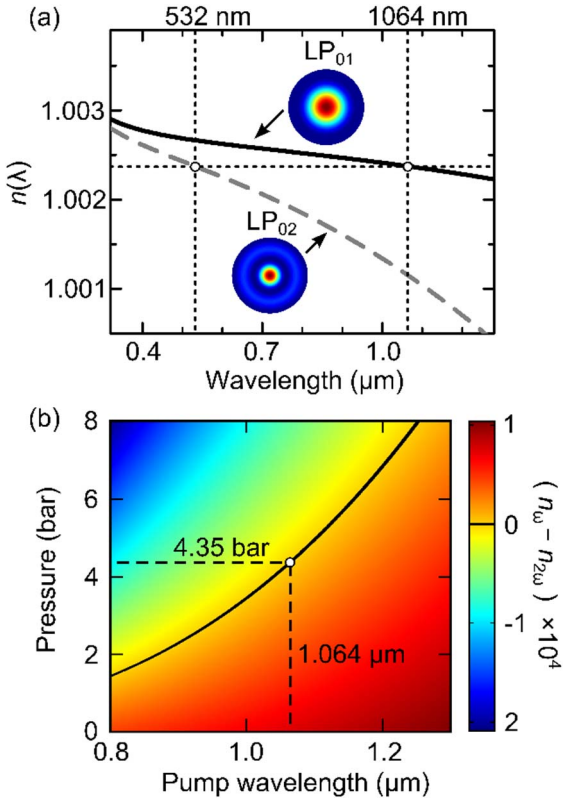

Fig. 1. (a) Wavelength dependence of the modal refractive indices of the LP_{01} and LP_{02} modes in a 4.5 bar, Xe-filled kagomé PCF, calculated analytically using the model in [13], assuming a flat-to-flat core diameter of 33.4 μm, a core wall thickness of 190 nm, and an s-parameter of 0.09. The refractive index of xenon was taken from [14]. Phase-matching conditions are satisfied for a pump wavelength of 1064 nm and the SH at 532 nm (dotted lines). The insets show the calculated transverse spatial intensity pattern of the modes [15]. (b) Difference between the modal indices of the LP_{01} pump and the LP_{02} SH as a function of the pressure and pump wavelength. Phase-matching conditions are satisfied when $n\omega = n_2\omega$ (black curve). The point on the curve corresponds to the scenario in (a).

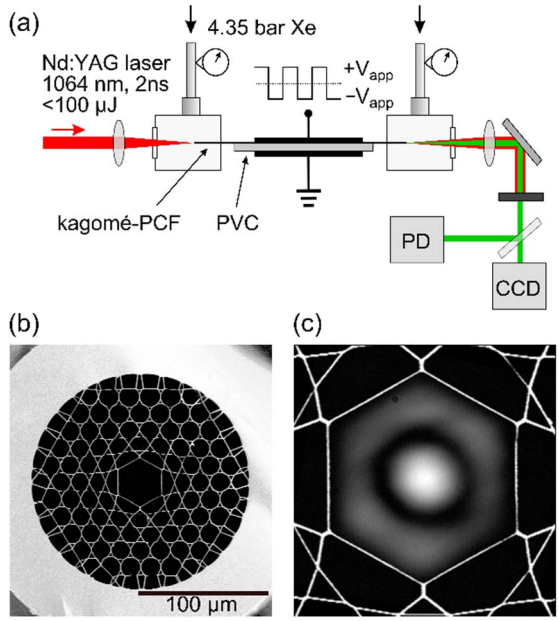

Fig. 2. (a) Schematic of the experimental setup. A square-wave ac voltage (amplitude ±1.8 kV and frequency 350 Hz) is applied across the Xe-filled kagomé PCF. A 1064 nm pump pulse in the LP_{01} mode generates an SH signal in the LP_{02} mode. PD, photodiode. (b) Scanning electron micrograph of the kagomé PCF. The flat-to-flat core diameter is 33.4 μm, and the thickness of the glass webs surrounding the core is 190 nm. The inner cladding is 170 μm in diameter, and the outer glass sheath is 47 μm thick. (c) Measured near-field intensity distribution (linear scale) of the SH signal at the fiber end face; it is clearly in the expected LP_{02} mode. An SEM image of the fiber core structure is superimposed for reference.

Pump pulses from a 1064 nm Nd:YAG microchip laser (duration 2 ns, repetition rate 1 kHz) were launched into the LP_{01} mode. At the output of the fiber, 532 nm dielectric bandpass filters were used to block the transmitted pump light, and the SH power and near-field modal pattern were monitored using a photodiode detector and a CCD camera. The measured SH modal profile corresponded, as expected, to the LP_{02} mode [see Fig. 2(c)].

The kagomé PCF used in the experiment was selected on the basis of its guiding properties, which featured relatively low propagation loss for the LP_{01} mode over a broad spectral region that included the pump frequency and its SH. The loss of the LP_{01} mode was measured by the cutback method to be 2 ± 0.5 dB/m, and that of the LP_{02} mode at 532 nm was estimated experimentally to be 13 ± 3 dB/m, using a novel technique that involved scanning a localized electric field along the fiber while monitoring the SH power (see last section for details).

We theoretically investigate the three-wave mixing interaction in the PCF leading to SH generation by solving the coupled nonlinear wave equations. The local electric field of the qth mode can be written as follows:

$$E_q = \frac{1}{2}\sqrt{\frac{2Z_0P_0}{n_q^g \iint e_q^2 \mathrm{d}x\mathrm{d}y}} b_q(z)e_q(x,y)e^{i(\beta_q z - qt)} + \text{c.c.}, \quad (1)$$

where $b_q(z)$ is its dimensionless, slowly varying amplitude and q is its angular frequency (ω for the pump mode and 2ω for the SH mode). $e_q(x,y)$ is its transverse field distribution and β_q is its propagation constant. Z_0 is the impedance of free space, P_0 is the input power, and n_q^g is the refractive index of the gas filling the hollow core (more than 99.8% of the light is in the core [2]). The field normalization implies that the power in the qth mode is $P_0|b_q(z)|^2$. Under the conditions of negligible pump attenuation and depletion, the differential equation for $b_{2\omega}$ can be written in the form:

$$\frac{\partial b_{2\omega}(z)}{\partial z} = i\kappa_{\text{eff}}^{(2)}|b_\omega^2| + (i\vartheta - \alpha_{2\omega})b_{2\omega}(z),$$
$$\kappa_{\text{eff}}^{(2)} = \frac{3\omega\chi^{(3)}QE_{\text{dc}}}{2cn_{2\omega}}\frac{\sqrt{2Z_0P_0n_{2\omega}^g}}{n_\omega^g}, \quad (2)$$

where c is the speed of light in the vacuum, $\alpha_{2\omega}$ is the amplitude loss coefficient of the LP_{02} SH mode, and ϑ is the dephasing parameter:

$$\vartheta = 2(n_\omega - n_{2\omega})\omega/c. \quad (3)$$

The overlap integral Q, which is calculated assuming that E_{dc} is constant throughout the core, takes the form:

$$Q = \frac{\iint e_\omega^2 e_{2\omega} \mathrm{d}x\mathrm{d}y}{\iint e_\omega^2 \mathrm{d}x\mathrm{d}y (\iint e_{2\omega}^2 \mathrm{d}x\mathrm{d}y)^{1/2}}, \quad (4)$$

where the integrals are over the transverse cross section. Q was evaluated using the analytical expressions for the modes in a capillary waveguide, and the results yielded a value of 28 mm^{-1} [15]. Note that although the linear overlap between the LP_{01} pump and LP_{02} SH modes is very small (they are almost orthogonal), the nonlinear overlap is much larger because the LP_{01} pump field is squared.

Equation (2) can be straightforwardly solved for $b_{2\omega}^2(z)$, assuming that $b_{2\omega}^2(0) = 0$. The energy W_{SH} converted to the SH from a single Gaussian pump pulse of energy W_P can then be written:

$$W_{SH} = W_P \frac{(\kappa_{eff}^{(2)} L)^2}{\sqrt{2}} \left| \mathrm{sinc}\left(\frac{(\vartheta + i\alpha_{2\omega})L}{2} \right) \right|^2 \exp(-\alpha_{2\omega} L), \quad (5)$$

where L is the nonlinear interaction length, and a quasi-CW approximation is used. Note that the actual SH energy measured will be slightly less owing to the attenuation in the 0.13 m-long un-poled fiber pigtail leading to the detector.

The SH signal was first monitored at several different Xe pressures close to the phase-matching point for a ±79 kV/cm, 350 Hz square-wave electric field and a launched pump pulse energy of 22 μJ. As expected, the data points [see Fig. 3(a)] follow a sinc^2 dependence on the pressure, and the SH signal peaks at 4.35 bar, as predicted in Fig. 1(b). The slight asymmetry in the second-harmonic generation signal, which is particularly noticeable when comparing the sidelobe amplitudes at 4.07 and 4.61 bar, is due to the linear dependence of the third-order susceptibility to the pressure.

Next, the dependence of the SH power on the pump energy and applied electric field strength was explored, keeping the pressure fixed at 4.35 bar. Again, as expected, the second-harmonic generation signal [see Fig. 3(b)] follows a quadratic dependence on the pump energy, with the square-wave electric field amplitude fixed at ±79 kV/cm. A similar dependence [see Fig. 3(c)] is seen when the electric field is varied, keeping the pump pulse energy constant at 29 μJ. This yields a normalized conversion efficiency of $5 \times 10^{-10}\%\ \mathrm{W}^{-1}\ \mathrm{cm}^{-1}$. No saturation effects were observed at the maximum values of the pump energy and bias field available in the experimental setup. This suggests that higher conversion efficiencies could be obtained if these parameters were scaled, for example, by using microelectrodes built into the fiber [16] or higher pulse energies.

Excellent fits to the theory (see the curves in Fig. 3) are obtained for values of E_{dc} that are 0.56 times smaller than estimated in the experiment. This disparity was much more pronounced for a constant dc poling field, where the SH signal dropped almost to zero after only a few seconds, suggesting that the dc field in the core is screened by space charges that accumulate somewhere in the system. This is, however, an artifact of the experiment, and does not affect the main conclusions of the current work.

The broad window of transparency offered by the kagomé PCF and other species of anti-resonant reflecting hollow-core

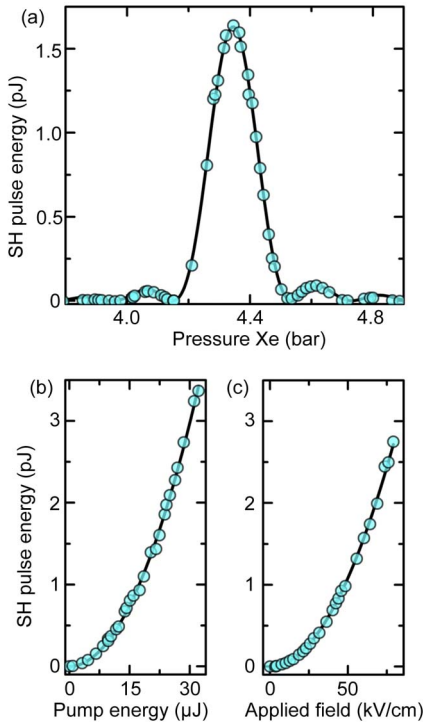

Fig. 3. Dots are data points, and the curves are theoretical fits, taking account of the increase in $\chi^{(3)}$ with pressure (see text). (a) Measured SH pulse energy as a function of the Xe pressure. The interaction length was 16 cm, the applied field was ±79 kV/cm, and the pump pulse energy was 22 μJ. The conversion efficiency is maximum at 4.35 bar, as predicted (see text). (b) SH pulse energy as a function of the pump energy at 4.35 bar and ±79 kV/cm. (c) SH pulse energy as a function of the applied field at 4.35 bar and 29 μJ pump energy. In both (b) and (c), the SH signal follows a quadratic dependence, in good agreement with theory [see Eq. (5)].

PCFs [1,17–19] allows light to be generated at experimentally challenging wavelengths, for example, in the ultraviolet or the terahertz regions. Also, the low dispersion of the refractive index means that the pumped SH phase mismatch varies slowly with the wavelength. For example, for a fixed xenon pressure of 4.35 bar and a nonlinear interaction length of $L = 16$ cm, the SH signal can be tuned over ~6 nm (FWHM) by tuning the pump over 12 nm. The conversion efficiency itself can of course be increased by using pulses with higher intensities.

A pair of gold electrodes could be incorporated into the hollow channels on opposite sides of the hollow core using established, selective melt-filling techniques [16]. The reduced electrode spacing would lower the required voltage and result in a much more compact device. Smaller core diameters would not only increase the Q, but also allow phase matching at a higher Xe pressure, thus increasing the effective value of $\chi^{(3)}$. Furthermore, since kagomé-style PCFs feature a high damage threshold, much higher than in solid glass-core fibers, and have a wide phase-matching bandwidth due to their weak dispersion, they would allow for the frequency doubling of very intense few-cycle pulses.

Implementing these improvements could lead to an increase in the SH conversion efficiency of several orders of

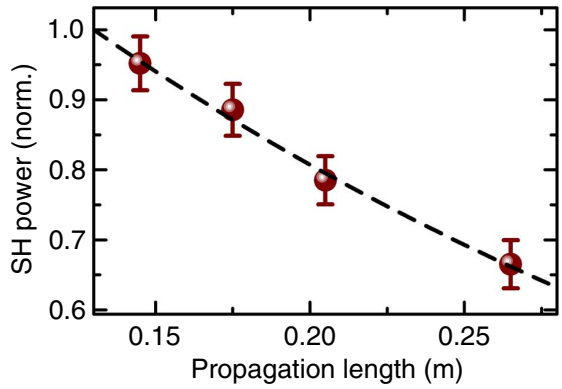

Fig. 4. SH signal in the LP_{02} mode at 532 nm generated with 2 cm-long electrodes placed at four different positions and measured as a function of the propagation length, which is the distance from the center of the poled section to the fiber output end. The fit to the data (dashed curve) yields 13 ± 3 dB/m at 532 nm.

magnitude, potentially approaching the efficiencies demonstrated in poled solid-core fibers, which can be as high as $\sim 0.001\%\ W^{-1}\ cm^{-1}$ [20].

Finally, pressure-tunable quasi-phase-matched (QPM) conversion between the LP_{01} modes at both the pump and SH frequencies can be arranged if a periodic electrode is used. For example, a QPM period of ~2 mm and a Xe pressure of 3.5 bar would allow phase-matched all-LP_{01} SH generation from 1064 to 532 nm. Higher conversion efficiencies could be obtained by raising the pressure; for example, a QPM period of ~1 mm would allow phase matching at a Xe pressure of 20 bar. This QPM period is much longer than in conventional single-mode fibers (where a few 10 s of micrometers is typical), facilitating electrode fabrication.

The setup may be used to characterize the propagation loss of the LP_{02} mode at 532 nm. For example, by applying a voltage sequentially to 2 cm-long electrodes placed at four different positions along the kagomé-PCF, and measuring the SH signal (see Fig. 4), it is straightforward after data processing to extract the propagation loss, which turns out to be 13 ± 3 dB/m. There is good agreement between this value and that previously measured in the kagomé PCF using a combination of prism-assisted side-coupling (to excite the selected mode) and cutback measurements [21,22].

The loss of the LP_{01} mode at the SH frequency could also be measured using a periodic electrode (see above), offering a compelling, noninvasive alternative to the cutback method. Used in combination with a tunable pump laser, the system would allow characterization over a broad bandwidth of the loss of the LP_{01} mode (and some higher modes) in any type of hollow-core PCF that guides at the pump and SH frequencies. This is especially interesting since the technique does not require an external optical source emitting in the difficult-to-access deep and vacuum UV regions. Moreover, in contrast to the common cutback method, the technique is nondestructive, and its accuracy is not affected by the quality of the fiber cleaves.

In conclusion, a phase-matched SH signal at 532 nm can be generated in the LP_{02} mode by applying a dc electric field across a Xe-filled, hollow-core kagomé PCF and pumping in the LP_{01} mode at 1064 nm. A particularly attractive feature of the system is that it is pressure tunable. Excellent agreement is obtained between the experimental results and the analytical expressions derived using the coupled-mode theory. Much higher SH conversion efficiencies are expected if electrodes are built into the PCF, or if fibers with a smaller core diameter are used, thus allowing for higher intensities per watt and phase-matching pressures. Quasi-phase matching by means of a periodic electrode would allow pressure-tunable phase matching between LP_{01} modes at both frequencies. The system has important potential applications in the noninvasive measurement of propagation losses at difficult-to-access frequencies (e.g., in the deep UV region) in hollow-core PCFs. It could also prove useful for frequency doubling ultrashort pulses with extremely high peak powers.

Acknowledgment. We thank B. M. Trabold, N. N. Edavalath, O. Bittel, and M. Lothar for their technical assistance and for the useful discussions.

REFERENCES

1. P. St.J. Russell, P. Holzer, W. Chang, A. Abdolvand, and J. C. Travers, Nat. Photonics **8**, 278 (2014).
2. J. C. Travers, W. Chang, J. Nold, N. Y. Joly, and P. St.J. Russell, J. Opt. Soc. Am. B **28**, A11 (2011).
3. F. Couny, F. Benabid, P. J. Roberts, P. S. Light, and M. G. Raymer, Science **318**, 1118 (2007).
4. N. Y. Joly, J. Nold, W. Chang, P. Hölzer, A. Nazarkin, G. K. L. Wong, F. Biancalana, and P. St.J. Russell, Phys. Rev. Lett. **106**, 203901 (2011).
5. D. P. Shelton, Phys. Rev. A **42**, 2578 (1990).
6. D. Milam and M. J. Weber, J. Appl. Phys. **47**, 2497 (1976).
7. P. Hölzer, W. Chang, J. C. Travers, A. Nazarkin, J. Nold, N. Y. Joly, M. F. Saleh, F. Biancalana, and P. St.J. Russell, Phys. Rev. Lett. **107**, 203901 (2011).
8. F. Belli, A. Abdolvand, W. Chang, J. C. Travers, and P. St.J. Russell, Optica **2**, 292 (2015).
9. F. Tani, F. Belli, A. Abdolvand, J. C. Travers, and P. St.J. Russell, Opt. Lett. **40**, 1026 (2015).
10. F. Emaury, C. J. Saraceno, B. Debord, D. Ghosh, A. Diebold, F. Gèrôme, T. Südmeyer, F. Benabid, and U. Keller, Opt. Lett. **39**, 6843 (2014).
11. P. G. Kazansky, P. St.J. Russell, and H. Takebe, J. Lightwave Technol. **15**, 1484 (1997).
12. R. H. Stolen and H. W. K. Tom, Opt. Lett. **12**, 585 (1987).
13. M. A. Finger, N. Y. Joly, T. Weiss, and P. St.J. Russell, Opt. Lett. **39**, 821 (2014).
14. A. Börzsönyi, Z. Heiner, M. P. Kalashnikov, A. P. Kovács, and K. Osvay, Appl. Opt. **47**, 4856 (2008).
15. E. A. J. Marcatili and R. A. Schmeltzer, Bell Syst. Tech. J. **43**, 1783 (1964).
16. H. W. Lee, M. A. Schmidt, R. F. Russell, N. Y. Joly, H. K. Tyagi, P. Uebel, and P. St.J. Russell, Opt. Express **19**, 12180 (2011).
17. F. Yu, W. J. Wadsworth, and J. C. Knight, Opt. Express **20**, 11153 (2012).
18. A. N. Kolyadin, A. F. Kosolapov, A. D. Pryamikov, A. S. Biriukov, V. G. Plotnichenko, and E. M. Dianov, Opt. Express **21**, 9514 (2013).
19. F. Poletti, Opt. Express **22**, 23807 (2014).
20. V. Pruneri, G. Bonfrate, P. G. Kazansky, D. J. Richardson, N. G. Broderick, J. P. de Sandro, C. Simonneau, P. Vidakovic, and J. A. Levenson, Opt. Lett. **24**, 208 (1999).
21. B. M. Trabold, D. Novoa, A. Abdolvand, and P. St.J. Russell, Opt. Lett. **39**, 3736 (2014).
22. J.-M. Ménard, B. M. Trabold, A. Abdolvand, and P. St.J. Russell, Opt. Express **23**, 895 (2015).